Mutagenesis of Specific Amino Acids Converts Carnitine Acetyltransferase into Carnitine Palmitoyltransferase[†]

Antonio G. Cordente,[‡] Eduardo López-Viñas,[§] María Irene Vázquez,[‡] Paulino Gómez-Puertas,[§] Guillermina Asins,[‡] Dolors Serra,[‡] and Fausto G. Hegardt*,[‡]

Department of Biochemistry and Molecular Biology, School of Pharmacy, University of Barcelona, E-08028 Spain, and Centro de Biología Molecular "Severo Ochoa", Consejo Superior de Investigaciones Científicas, Cantoblanco, E-28049 Madrid, Spain

ABSTRACT: Carnitine acyltransferases catalyze the exchange of acyl groups between carnitine and CoA. The members of the family can be classified on the basis of their acyl-CoA selectivity. Carnitine acetyltransferases (CrATs) are very active toward short-chain acyl-CoAs but not toward medium- or long-chain acyl-CoAs. Previously, we identified an amino acid residue (Met[564] in rat CrAT) that was critical to fatty acyl-chain-length specificity. M564G-mutated CrAT behaved as if its natural substrates were medium-chain acyl-CoAs, similar to that of carnitine octanoyltransferase (COT). To extend the specificity of rat CrAT to other substrates, we have performed new mutations. Using in silico molecular modeling procedures, we have now identified a second putative amino acid involved in acyl-CoA specificity (Asp[356] in rat CrAT). The double CrAT mutant D356A/M564G showed 6-fold higher activity toward palmitoyl-CoA than that of the single CrAT mutant M564G and a new activity toward stearoyl-CoA. We show that by performing two amino acid replacements a CrAT can be converted into a pseudo carnitine palmitoyltransferase (CPT) in terms of substrate specificity. To change CrAT specificity from carnitine to choline, we also prepared a mutant CrAT that incorporates four amino acid substitutions (A106M/T465V/T467N/R518N). The quadruple mutant shifted the catalytic discrimination between L-carnitine and choline in favor of the latter substrate and showed a 9-fold increase in catalytic efficiency toward choline compared with that of the wild-type. Molecular in silico docking supports kinetic data for the positioning of substrates in the catalytic site of CrAT mutants.

Carnitine acyltransferases catalyze the exchange of acyl groups between carnitine and CoA, and play a central role in fatty acid metabolism in eukaryotes. There are three carnitine acyltransferase families that differ in their acyl-chain-length selectivity: carnitine palmitoyltransferases (CPTs[1]), CPT I, and CPT II catalyze long-chain fatty acids, and carnitine octanoyltransferase (COT) prefers medium-chain fatty acids, whereas carnitine acetyltransferase (CrAT) uses short-chain acyl-CoAs (*1*, *2*).

CPT I and CPT II are essential for mitochondrial β-oxidation and are located in the outer and inner mitochondrial membranes, respectively, facilitating the transfer of long-chain fatty acids from the cytoplasm to the mitochondrial matrix. CPT I is the rate-limiting step in β-oxidation (*3*).

COT is localized in peroxisomes and mediates the transport of medium-chain fatty acids from peroxisomes to mitochondria through the conversion of acyl-CoAs, shortened by peroxisomal β-oxidation, into acyl-carnitine (*4*). CrAT catalyzes the reversible conversion of acetyl-CoA and carnitine to acetylcarnitine and free CoA.

Because of the impermeability of organelle membranes to CoA, CrATs function in a compartmental buffering system by maintaining the appropriate levels of acetyl-CoA and CoA in cellular compartments. Mitochondrial CrAT plays a major role in modulating matrix acetyl-CoA concentration. The production and utilization of acetyl-CoA in the mitochondrial matrix occurs at a major metabolic crossroad. The regulation of the fate of acetyl-CoA is mediated, to a large extent, by the effects of the molecule itself on pyruvate dehydrogenase kinase, which is inhibited by a high acetyl-CoA/CoA ratio. In the liver, mitochondrial acetyl-CoA also activates the key gluconeogenic enzyme pyruvate carboxylase. Therefore, high rates of β-oxidation of fatty acids result in the activation of gluconeogenesis from pyruvate and its precursors (*5*). In mammalian tissues, CrATs can also contribute to the excretion of excess or harmful acyl molecules as acylcarnitines (*6*). CrATs also appear to play an important role in human health. For example, decreases in CrAT activity have been reported in patients with disorders of the nervous system, such as Alzheimer's disease (*7*), ataxic encephalopathy (*8*), and several vascular diseases (*9*, *10*). Moreover, it has been recently reported that hepatic overexpression of

* To whom correspondence should be addressed. Phone: +34 93 4024523. Fax: +34 93 4024520. E-mail: fgarciaheg@ub.edu and dserra@ub.edu.
[‡] University of Barcelona.
[§] Consejo Superior de Investigaciones Científicas.

[1] Abbreviations: CrAT, carnitine acetyltransferase; COT, carnitine octanoyltransferase; CPT, carnitine palmitoyltransferase; ChAT, choline acetyltransferase; wt, wild-type; 3-D, three-dimensional.

malonyl-CoA decarboxylase reverted muscle, liver, and whole-animal insulin resistance (*11*). These findings were accompanied by a marked decrease in β-hydroxybutyryl-carnitine in muscle samples. This was interpreted as an indication that an improvement of the mitochondrial function of insulin-resistant muscle impedes the accumulation of acetyl-CoA, thereby preventing ketogenesis. In these conditions, carnitine acetyltransferase can be critical because of its buffering action in maintaining the appropriate levels of acetyl-CoA and CoA.

The crystal structures of the mouse and human CrAT have been reported alone and in complex with their substrates carnitine or CoA (*12, 13*). The CrAT structure contains two domains that share the same backbone fold. The active site is located at the interface of the two domains, and carnitine and CoA are bound in a tunnel on opposite sides of the catalytic histidine residue. More recently, the 3-D structure of mouse COT (*14*) was reported, alone and in complex with the substrate octanoylcarnitine, showing for the first time, the structure of the acyl moiety binding site in the carnitine acyltransferase family. The overall structure of COT is very similar to that of CrAT, although there are significant differences in the acyl group binding region, which are responsible for the differing substrate specificities of the two enzymes.

We and others recently reported that a single amino acid determined the acyl-CoA substrate specificity of CrAT and COT (Met[564] and Gly[553], respectively) (*14−16*). We demonstrated, by kinetic experiments and 3-D models in rat CrAT, that the mutation of this voluminous methionine to the smaller glycine (CrAT M564G mutant) permits the access of medium-chain acyl-CoAs to the hydrophobic pocket (*15*). Data from the mouse CrAT M564G mutant crystal confirm our hypothesis because they reveal a deep acyl group binding pocket that can accommodate medium-chain acyl-CoAs (*16*). Surprisingly, rat CrAT mutant M564G was very active toward myristoyl-CoA but much less so toward palmitoyl-CoA, suggesting that other amino acids may be responsible for governing the access of acyl-CoAs longer than myristoyl-CoA.

Choline acetyltransferase (ChAT) belongs to the choline/carnitine acyltransferase family and catalyzes a reaction similar to that of CrAT except that the acetyl group from acetyl-CoA is transferred to choline instead of carnitine. The difference between these two substrates is that carnitine has an additional carboxymethyl group that replaces a hydrogen at C_1 of the choline. The recent publication of the rat ChAT crystal (*17, 18*) and several mutagenesis studies (*19−21*) have led to a model for choline/carnitine discrimination in ChAT on the basis of both electrostatic and steric factors. In the former, two of the residues that play critical roles in rat CrAT by electrostatically interacting with the carboxylate group of carnitine, Thr[465], and Arg[518] are replaced by neutral amino acids (Val[459] and Asn[514]) in rat ChAT. Both residues were mutated by Cronin (*19*) in rat ChAT to their counterparts in CrAT (V459T and N514R), and the resulting ChAT mutant showed an increase in catalytic efficiency toward carnitine. In addition to electrostatic factors, the crystal data also indicate that steric factors might contribute to the selectivity of ChAT toward choline rather than carnitine.

In the present study, we have identified a new amino acid (Asp[356] in rat CrAT) that could contribute, along with Met[564],

to acyl-CoA selectivity in CrAT. Enzyme activity and kinetic parameters of the yeast-expressed rat CrAT double mutant D356A/M564G show that it has a preference for palmitoyl-CoA as the substrate rather than its natural substrate acetyl-CoA. Furthermore, to redesign rat CrAT specificity from carnitine to choline, we replaced four amino acids in rat CrAT with their counterparts in ChAT (A106M, T465V, T467N, and R518N) by site-directed mutagenesis. The modified CrAT shows an increase in catalytic efficiency toward choline and a decrease in catalytic efficiency toward carnitine compared with that of the wt enzyme.

EXPERIMENTAL PROCEDURES

Construction of Rat CrAT and CPT I Models. A structural model of wt CrAT enzyme was constructed by homology modeling techniques using as templates the structures deposited in the Protein Data Bank (pdb) corresponding to human (1NM8) (*13*) and mouse CrAT (1NDB, 1NDF, and 1NDI) (*12*), essentially as described elsewhere (*15*). The model of liver CPT I (L-CPT I) was constructed using as a template the structure of mouse carnitine octanoyltransferase (1XL7, 1XL8) (*14*), essentially as described elsewhere (*22*). CrAT mutants M564G, D356A/M564G, T465V/T467N/R518N, and A106M/T465V/T467N/R518N were modeled by the same procedures using the rat wt CrAT model as the template. The structural quality of the models was checked using the WHAT-CHECK routines (*23*) from the WHAT IF program (*24*) and the PROCHECK validation program from the SWISS-MODEL server facilities (*25*). The 3-D coordinates of the rat ChAT structure were obtained from the pdb entries 1Q6X (*17*) and 1T1U (*18*).

Molecular Docking. Structural models of the molecular interaction between the substrates myristoyl-CoA (C_{14}-CoA), palmitoyl-CoA (C_{16}-CoA), stearoyl-CoA (C_{18}-CoA), and arachidoyl-CoA (C_{20}-CoA) and the 3-D models of the putative receptor mutant proteins of rat CrAT M564G and D356A/M564G were built using the suite of programs included in the Autodock package (*26, 27*). The proteins and acyl-CoA ligands were prepared using standard procedures as specified in the package documentation. To ensure a complete search of binding sites available for acyl-CoAs, independent docking calculations were performed. To intensively sample their conformational space, we used the whole set of rotatable bonds in the acyl chains of the ligands. Only docking models with their CoA residue positions close to those found in the 1NDI crystal (*12*) were considered for further steps. Finally, among the position clusters selected for each ligand, the model with the lowest docking energy for each particular interaction was considered. The putative palmitoyl-CoA binding site in rat wt L-CPT I was modeled on the basis of information from the docking procedures using the AutoDock docking program, essentially as described elsewhere (*22*). The structural interactions between the substrates choline and carnitine and the rat wt ChAT, wt CrAT, and CrAT mutant proteins T465V/T467N/R518N (triple mutant, TM) and A106M/T465V/T467N/R518N (quadruple mutant, QM), respectively, were performed using the methods implemented in the Autodock suite. To preserve the structural position and conformation of carnitine and choline, respectively, within the active sites indicated in the original publications of CrAT and ChAT structures (*12, 17, 18*), rigid docking models were obtained for every putative

interaction. Only docked models locating the common trimethylammonium group of both choline and carnitine in the sites originally suggested were considered for refining. As in the case of the acyl-CoA substrates, the lowest energy docked models were selected within the filtered sets.

Construction of Site-Directed Mutants of Rat CrAT. Plasmids pYESCrAT^{M564G} and pGEX-CrAT^{wt} were obtained as previously described (*15*). CrAT mutant D356A/M564G was constructed using the Quick Change PCR-based mutagenesis procedure (Stratagene) with the pYESCrAT^{M564G} plasmid as the template. CrAT mutant T465V/T467N was obtained using the pGEX-CrAT^{wt} plasmid as the template; CrAT mutant T465V/T467N/R518N was constructed using the pGEX-CrAT$^{T465V/T467N}$ plasmid as the template and CrAT mutant A106M/T465V/T467N/R518N was constructed using the pGEX-CrAT$^{T465V/T467N/R518N}$ plasmid as the template. The appropriate substitutions as well as the absence of unwanted mutations were confirmed by sequencing the inserts.

Expression of Rat CrAT and L-CPT I in Saccharomyces cerevisiae. Plasmids containing wt L-CPT I and CrAT mutants M564G and D356A/M564G were expressed in yeast cells, and mitochondrial cell extracts were prepared as previously described (*28*). A *S. cerevisiae* strain devoid of COT and CPT activity and lacking the endogenous CAT2 gene (FY23Δ*cat2* (MATa trp1 ura3 Δ*cat2*::LEU2)) was used as an expression system (*29*).

Expression and Purification of Rat CrAT in Escherichia coli. For expression and purification of rat CrAT wt and CrAT triple mutant T465V/T467N/R518N and quadruple mutant A106M/T465V/T467N/R518N, the glutathione S-transferase (GST) gene fusion system (Amersham Biosciences) was used. The pGEX-6P-1 plasmids containing wt CrAT and mutant CrAT were transformed into *E. coli* BL21, and fusion protein GST-CrAT was overexpressed overnight after the addition of 0.1 mM of isopropyl-1-thio-β-D-galactopyranoside (IPTG) at 18 °C. The soluble fusion protein was purified from bacterial lysates using glutathione-sepharose 4B with a batch method. Finally, CrAT was eluted by cleavage of the fusion protein with the site-specific protease PreScission protease. The eluted protein contains five additional amino acids (Gly-Pro-Leu-Gly-Ser) at its *N*-terminus before the ATG start codon.

Determination of Enzymatic Activity. Two methods were used for the assay of carnitine acyltransferase: an endpoint fluorometric method (*30*) and a radiometric method (*28*). The fluorometric assay was used in all cases, unless otherwise indicated.

Fluorometric Method. The forward reaction of carnitine acyltransferase activity was assayed for 8 min at 30 °C in a solution containing 0.1 mM acyl-CoA, 1.5 mM EDTA, 1.5 mM L-carnitine, and 40 mM Hepes buffer at pH 7.8, in a total volume of 600 μL. The reactions were started by the addition of 5 μg of yeast-expressed CrAT or from 0.1 to 1 μg of *E. coli*-expressed CrAT. Parallel (blank) assays were run in the absence of L-carnitine or choline. All fluorometer recordings were performed with a Perkin-Elmer LS 45 luminescence spectrometer, and the enzyme activities were measured in duplicate. For the determination of the K_m value for carnitine or choline, acyl-CoA was fixed at 0.1 mM. For the determination of the K_m value for acyl-CoA, the choline concentration was fixed at 100 mM, and the carnitine concentration was fixed at 1.5 mM (wt and CrAT mutant

D356A/M564G) or 100 mM (CrAT triple mutant T465V/T467N/R518N and quadruple mutant A106M/T465V/T467N/R518N). Carnitine was neutralized with KOH before use. The values reported are the means and standard deviations of three determinations. Protein concentrations were measured using the Bio-Rad protein assay with BSA as standard. The K_m and V_{max} values were determined by fitting the data using nonlinear regression analysis to the Michaelis–Menten equation with Sigma Plot software. Catalytic efficiency was defined as V_{max}/K_m for yeast-expressed CrAT and as the K_{cat}/K_m for *E. coli*-expressed CrAT.

Radiometric Method. This assay was used to compare CrAT double mutant D356A/M564G and L-CPT I wild-type activities in mitochondria-enriched fractions (5 μg) obtained from yeast. The forward reaction of carnitine acyltransferase activity was assayed for 4 min at 30 °C in a total volume of 200 μL as previously described (*28*). The substrates were 400 μM L-[*methyl*-³H]carnitine and 50 μM acyl-CoAs of varying length, ranging from hexanoyl-CoA (C_6-CoA) to arachidoyl-CoA (C_{20}-CoA).

Immunological Techniques. The mitochondrial protein (8 μg) from *S. cerevisiae* expressing CrAT was treated with the sample buffer and subjected to 8% (w/v) SDS–PAGE. Electroblotting to nitrocellulose sheets was carried out for 1 h at 250 mA. The immunodetection of CrAT was performed using anti-rat CrAT antibodies (1:10 000 dilution) (*15*). The blots were developed with the ECF Western blotting system (Amersham Biosciences). The quantifications were carried out using a fluorescence scanning device from Molecular Dynamics Storm 840.

RESULTS AND DISCUSSION

Re-Engineering CrAT into a Pseudo CPT. In an earlier study, we showed that the amino acid Met^{564} of rat CrAT was critical to fatty acyl-chain-length specificity in CrAT (*15*) because its mutation to glycine (CrAT mutant M564G) broadened CrAT acyl-CoA specificity from short-chain acyl-CoAs to medium-chain acyl-CoAs; indeed, we transformed rat CrAT into a pseudo COT. We also constructed a 3-D model of the location of fatty acyl-CoAs in the active center of wt and mutated M564G CrAT. After a thorough examination of the 3-D model for the positioning of myristoyl-CoA in the CrAT M564G mutant, we identified one charged residue, Asp^{356}, which conforms the putative bottom closure of the hydrophobic pocket that could sterically hinder the correct positioning of longer acyl-CoAs than myristoyl-CoA, such as palmitoyl-CoA. To create a more suitable environment for the acyl group of long-chain acyl-CoAs inside the hydrophobic pocket of CrAT, we mutated Asp^{356} to the small, uncharged hydrophobic residue Ala. We prepared the double CrAT mutant D356A/M564G, which was expressed in a *S. cerevisiae* strain devoid of endogenous CrAT, COT, and CPT activity. Enzyme activity of the yeast-expressed CrAT mutant D356A/M564G was tested for acyl-CoA substrates of various lengths from acetyl-CoA to arachidoyl-CoA and compared with that of the CrAT mutant M564G. As previously described (*15*), CrAT mutant M564G (Table 1) was very active toward medium-chain acyl-CoAs, especially hexanoyl-CoA, but much less active toward palmitoyl-CoA (802 and 18.0 nmol·min⁻¹·mg protein⁻¹, respectively), and its activity with longer acyl-CoAs (stearoyl- and arachidoyl-CoA) was

Table 1: Enzyme Activities of Rat CrAT wt and Mutants M564G and D356A/M564G Expressed in *Saccharomyces cerevisiae*[a]

acyl-CoA	activity (nmol·min^{-1}·mg protein^{-1})		
	CrAT wt	CrAT M564G	CrAT D356A/M564G
C_2-CoA	409 ± 48	234 ± 30	50.7 ± 4.0
C_4-CoA	518 ± 19	641 ± 3.2	138 ± 26
C_6-CoA	138 ± 15	802 ± 66	246 ± 15
C_8-CoA	61 ± 1.1	488 ± 24	127 ± 29
C_{10}-CoA	20.7 ± 5.7	136 ± 7.3	67.0 ± 0.7
C_{12}-CoA	6.0 ± 2.6	350 ± 5.0	150 ± 24
C_{14}-CoA	0.33 ± 0.07	409 ± 29	218 ± 9.0
C_{16}-CoA	UD	18.0 ± 3.6	100 ± 19
C_{18}-CoA	UD	UD	38.9 ± 1.4
C_{20}-CoA	UD	UD	UD

[a] The mitochondrial protein from yeast expressing wt CrAT and CrAT mutants M564G and D356A/M564G were assayed with acyl-CoAs of different carbon length ranging from C_2-C_{20} as described in Experimental Procedures. The results are the mean $\pm$ SD of at least three independent experiments with different preparations. UD represents the undetectable activity.
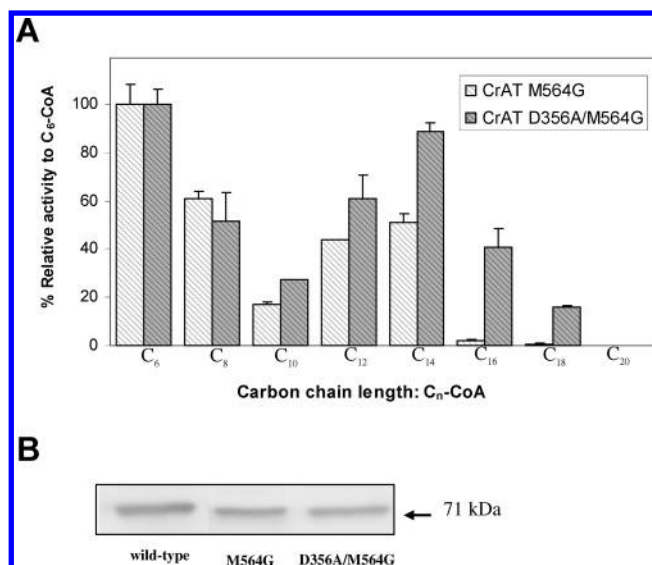

FIGURE 1: Carnitine acetyltransferase activity of *S. cerevisiae* cells expressing CrAT mutant M564G and double mutant D356A/M564G. (A) Extracts from yeast expressing CrAT mutant M564G and double mutant D356A/M564G were assayed for activity with acyl-CoAs of different chain length ranging from C_6-C_{20}, as described in Experimental Procedures. The results are expressed as the relative acyl-CoA activity with regard to hexanoyl-CoA activity (scaled to 100). The results are the mean $\pm$ SD of at least three independent experiments with different preparations. (B) Immunoblots showing expression of wt CrAT, CrAT M564G, and CrAT D356A/M564G. *S. cerevisiae* extracts (8 μg) were separated by SDS−PAGE and subjected to immunoblotting using specific antibodies. The arrows indicate the migration position and the molecular mass of rat CrAT (71 kDa).

undetectable. CrAT double mutant D356A/M564G also showed maximum activity toward hexanoyl-CoA (246 nmol·min^{-1}·mg protein^{-1}), but in contrast, it showed a 6-fold increase in activity toward palmitoyl-CoA (100 nmol·min^{-1}·mg protein^{-1}) and a new activity toward stearoyl-CoA (38.9 nmol·min^{-1}·mg protein^{-1}) compared with that of the single mutant M564G. If we express the results for palmitoyl-CoA as its relative activity with respect to hexanoyl-CoA, this figure was 41% for the CrAT double mutant but only 2% for the single mutant (Figure 1A).
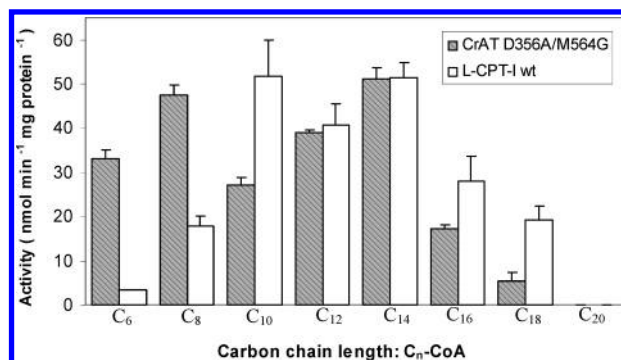

FIGURE 2: Carnitine acyltransferase activity of *S. cerevisiae* cells expressing L-CPT I wild type and CrAT double mutant D356A/M564G. The mitochondrial protein from yeast expressing L-CPT I and CrAT double mutant D356A/M564G were assayed for activity using a radiometric method with acyl-CoAs of different chain length ranging from C_6-C_{20}, as described in Experimental procedures. The results are the mean $\pm$ SD of at least three independent experiments with different preparations.

Table 2: Kinetic Parameters of Rat CrAT Mutant D356A/M564G Expressed in *Saccharomyces cerevisiae*[a]

acyl-CoA	K_m (μM)	V_{max} (nmol·min^{-1}·mg protein^{-1})	catalytic efficiency (V_{max}/K_m)
C_2-CoA	23.0 ± 3.1	66.5 ± 2.1	2.9
C_{16}-CoA	7.2 ± 0.4	138 ± 25	19.2

[a] Mitochondrial protein from yeast expressing CrAT mutant D356A/M564G was assayed with acetyl- and palmitoyl-CoA, as described in Experimental Procedures. The results are the mean $\pm$ SD of at least three independent experiments with different preparations.

In addition, yeast-expressed CrAT double mutant D356A/M564G and L-CPT I wt activities were compared using a radiometric method with acyl-CoAs of different length from C_6-CoA to C_{20}-CoA (Figure 2). The CrAT double mutant showed exactly the same activity as that of L-CPT I when C_{12}-CoA and C_{14}-CoA were used as substrates. In longer acyl-CoAs, the CrAT double mutant displayed a similar activity toward palmitoyl-CoA, approximately 65% of that of L-CPT I wt (17.8 vs 28 nmol·min^{-1}·mg protein^{-1}, respectively), whereas its activity with stearoyl-CoA was 25% of that of L-CPT I wt. The CrAT double mutant still maintained strong activity with C_6 and C_8-CoA as substrates, whereas the L-CPT I activity toward acyl-CoAs with fewer than 10 carbons in their chain was much lower.

These results indicate that the replacement of Asp[356], which conforms the bottom closure of the acyl-CoA binding pocket of CrAT by alanine (D356A) along with the mutation of Met[564] to Gly, allows CrAT to catalyze long-chain acyl-CoAs such as palmitoyl- and stearoyl-CoA. CrAT double mutant D356A/M564G catalyzes acyl-CoAs of a wide range of chain length, from acetyl-CoA to stearoyl-CoA.

Moreover, we determined the kinetic parameters of the CrAT mutant D356A/M564G with its novel substrate palmitoyl-CoA and its natural substrate acetyl-CoA (Table 2). The mutant showed standard saturation kinetics for both acyl-CoAs. The K_m values with acetyl-CoA and palmitoyl-CoA were 23 and 7.2 μM, respectively, indicating a preference for long-chain acyl-CoAs. Furthermore, the K_m value of this double mutant with palmitoyl-CoA was very similar to that of L-CPT I wt, 5.7 μM (22). When acetyl-CoA was the substrate, the catalytic efficiency (defined as V_{max}/K_m ratio)
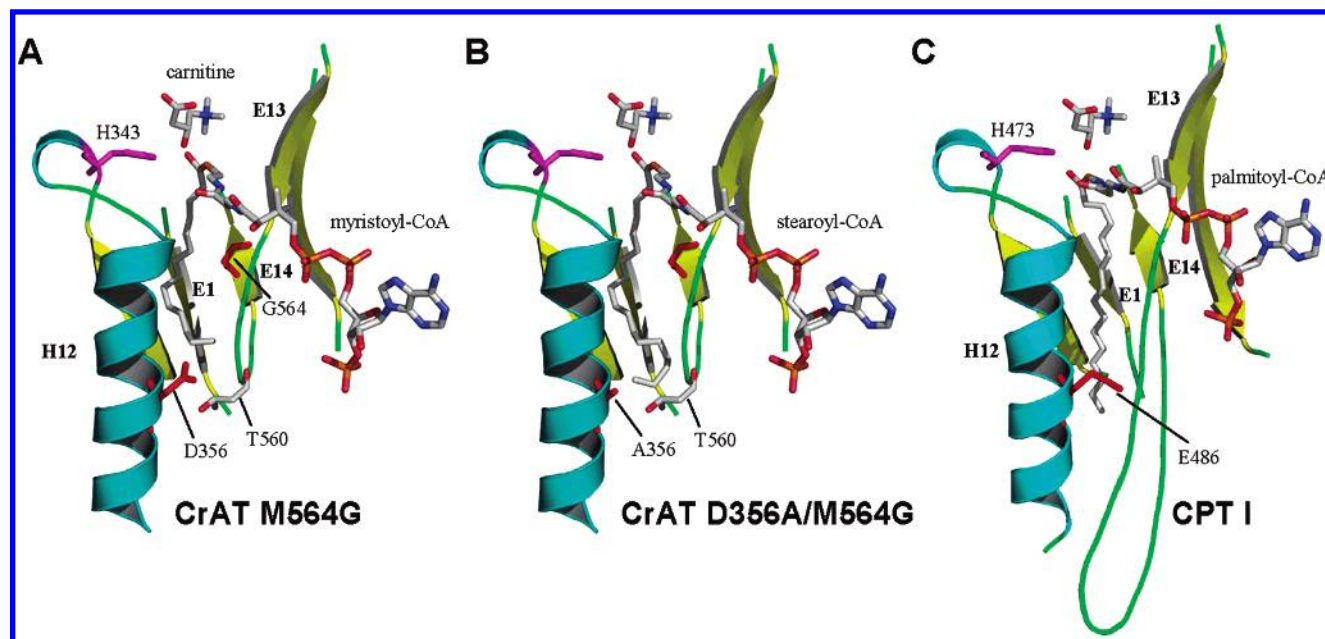
FIGURE 3: Proposed models for the positioning of long-chain acyl-CoAs in CrAT mutants M564G and D356A/M564G and wt L-CPT I. (A) Location of a myristoyl-CoA molecule in the pocket opened in CrAT mutant M564G. (B) Location of a stearoyl-CoA molecule (showing a U-turn of the ending carbon atom bonds) in the deep pocket open in CrAT mutant D356A/M564G. The position of residues Gly[564] and Asp[356] or Ala[356] (red) as well as Thr[560], the catalytic His[343] (magenta), and the molecule of carnitine are indicated. Secondary structure elements of the active center surrounding the acyl chain locus are also represented (alpha helix H12 in blue, beta strands in yellow). (C) Model for the location of a molecule of palmitoyl-CoA in CPT I. The presence of charged Glu[486] does not interfere with the substrate position because of the wider cavity conformed by the naturally adopted structural elements, including the distinctive long and flexible loop between beta strands E13 and E14.

was 2.9, whereas with palmitoyl-CoA, it was 19.2, which again shows that the double CrAT mutant prefers long-chain acyl-CoAs. Western blot of yeast-expressed wt CrAT and mutants D356A/M564G and M564G showed the same molecular masses and similar expression levels (Figure 1B).

Positioning of Long-Chain Acyl-CoAs in CrAT Mutant D356A/M564G. In a previous study (15), a 3-D model was proposed for the location of myristoyl-CoA in the hydrophobic pocket of the CrAT single mutant M564G. Refined in silico docking techniques were used in the present study, allowing the free rotation of the acyl chain bonds of the ligands. This ensured a complete scan of the available conformational space inside the enzyme cavity. The new model for the position of myristoyl-CoA is similar to the published model (*15*), locating the acyl chain in the cavity that is open when Met[564] is replaced by glycine. The bottom of the pocket is defined by the presence of Thr[560], which closes the enzyme wall to the external surface and Asp[356], which prevents the correct positioning of acyl-CoAs longer than myristoyl-CoA (Figure 3A).

The bigger cavity formed in CrAT mutant D356A/M564G by replacing the larger, charged Asp[356] by the tiny, nonpolar alanine, allows the positioning of longer-chain acyl-CoAs. This has also been calculated, using the same in silico docking method, for palmitoyl-CoA (C_{16}-CoA) (data not shown) and stearoyl-CoA (C_{18}-CoA) (Figure 3B). The last four carbon atoms of the acyl chain of stearoyl-CoA form a U-turn, which avoids collision with Thr[560] at the bottom of the tunnel and accommodates them in the space available around the substituted Ala[356].

When the docking of very long-chain acyl-CoAs, such as arachidoyl-CoA (C_{20}-CoA), into the large cavity of the CrAT D356A/M564G mutant was carried out, no models with low

(stable) energy were obtained despite using the minimum constraints of the appropriate location of the substrate to the enzyme active center. This indicates that the available space was too small to accommodate acyl chains of more than 18 atoms in length. The U-turn formed by stearoyl-CoA points toward the residues in the alpha helix H12 (Figure 3B), leaving no free space for additional carbon atoms of longer acyl chains. The absence of an appropriate model is consistent with the lack of activity of the D356A/M564G mutant enzyme toward arachidoyl-CoA (Figure 1A).

Taking into account all of the previous results, we propose a model for the acyl-CoA chain-length discrimination in CrAT on the basis of the presence of two amino acids, Met[564] and Asp[356], which act as checkpoints at different stages of the entry of acyl-CoAs to the fatty acid binding site. The bulkier side chain of Met[564] forms the floor of the shallow fatty acid binding pocket of CrAT and impedes the entry of medium- and long-chain acyl-CoAs, which explains CrAT selectivity for short-chain acyl-CoAs. The replacement of this Met by the smaller Gly (M564G) opens the binding site and reveals a deeper hydrophobic pocket that can accommodate acyl-CoAs of up to 14 carbons. The hydrophobic chain of longer acyl-CoAs cannot fit in the pocket, in the presence of the side chain of charged Asp[356] and, therefore, cannot be catalyzed by the enzyme. The substitution of this amino acid by a smaller, noncharged residue (D356A) along with the M564G mutation, completely opens the binding site and allows the entry of long-chain acyl-CoAs, such as palmitoyl- and stearoyl-CoA.

It has to be noted that the replacement of Met[564] by Gly is based on both structural and sequence alignment considerations (Met is replaced by Gly in COTs and CPTs), and this substitution could be considered as an evolutionary
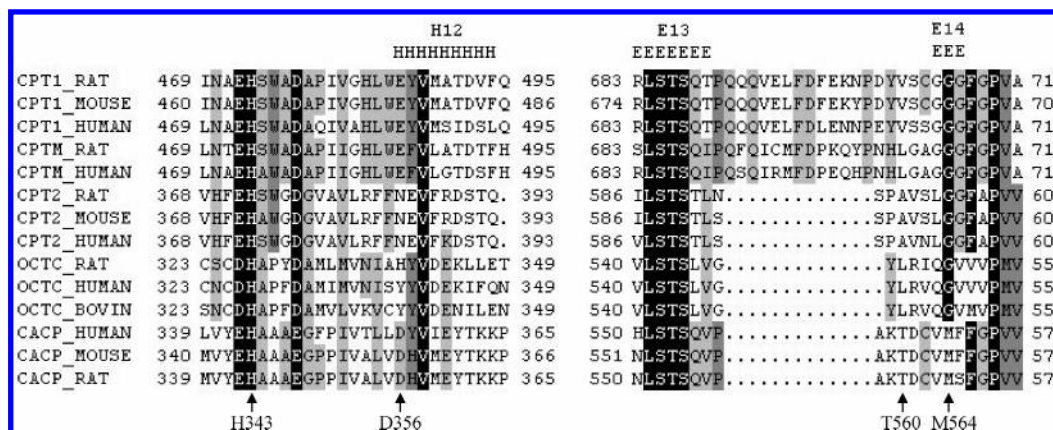
FIGURE 4: Alignment of representative sequences of structure elements surrounding the acyl chain locus of carnitine acyltransferases. The amino acid sequence of 14 representative enzymes that catalyze short acyl-CoAs as substrates: CrAT (CACP) from humans, mice, and rats; and enzymes which have medium- and long-chain acyl-CoAs as substrates: L-CPT I (CPT1) from rats, mice, and humans; M-CPT I (CPTM) from humans and rats; CPT II (CPT2) from rats, mice, and humans; and COT (OCTC) from humans, rats, and bovines were obtained from the SwissProt data bank and aligned using ClustalW. The residues are colored according to conservation. The CrAT Asp[356] residue corresponds to His or Tyr for COT (His[340] or Tyr[340]), and for CPT I, it is a glutamic (Glu[486]), and for CPT II, it is an asparagine (Asn[385]). The position of catalytic histidine (CrAT His[343]) and the conserved residue according to acyl-chain-length specificity (for CrAT, it is a methionine -Met[564]-, and for COT and CPTs, it is a glycine) are also noted. The secondary structure elements alpha helix H12 and beta strands E13 and E14 are indicated.

development that was selected because it enabled the carnitine acyltransferase family to catalyze longer acyl-CoAs. However, our replacement of the Asp[356] by Ala was only based on structural considerations. Alignment of the proteins of the family shows high variability in the zone close to the Asp[356], and the orthologous residues corresponding to CrAT Asp[356] are His/Tyr in COT, Asn in CPT II, and Glu in CPT I (Figure 4). In these enzymes, naturally conformed to accept long chain substrates, the cavity has adopted a shape slightly different to that of acetyltransferases. Small displacements of beta strands E1 and E13 as well as alpha helix H12 lead to a wider cavity where long substrates can adopt less restrictive conformations. This situation may be extrapolated from CPT I models (*22*), and it was observed in mouse COT structures (*14*). Therefore, the presence of bulky or charged residues in this position for long-chain enzymes is not so critical in terms of substrate fitting as it is for mutated carnitine acetyltransferases, which carry a narrower, hidden cavity. The mutation of Asp[356] to Ala along with the mutation of Met[564] to Gly creates an artificial enzyme that behaves as a CPT in terms of acyl-CoA specificity, although it is clear that the replacement of this Asp[356] by Ala is not the strategy followed by nature to handle long-chain substrates in CPTs, in contrast to the replacement of Met[564] by Gly. The selectivity for long-chain substrates may be determined by more complicated factors than specific amino acid variations between the different members of the family, possibly by the interactions among several different residues, and, at the same time, by variations in secondary structural elements. The most striking difference in the CPT I enzymes is the presence of a 13-amino acid insertion between beta strands E13 and E14 (Figure 4) that may form a more flexible pocket that can accommodate long-chain acyl groups (Figure 3C). Interestingly, this insertion is located just before the Met[564] residue.

As suggested by in silico modeling procedures, the cavity opened in the D356A/M564G mutant is almost completely occupied when stearoyl-CoA is introduced. Even allowing the full rotation of acyl chain bonds, it was impossible to obtain an active-enzyme compatible model for longer substrates. The longer substrates could perhaps be accommodated in the hydrophobic pocket if the side chain of Thr[560] were to be removed. However, the fact that this residue is part of the external surface of the protein introduces new variables (e.g., contacts of the end of the acyl chain with surrounding water), which makes it difficult to develop a model using current in silico methodologies.

Choline−Carnitine Discrimination in Rat CrAT. Taking into consideration all of the structural information revealed by the recent publication of the rat ChAT crystal (*17*, *18*) and the mutagenesis studies performed by Cronin (*19*), we attempted to redesign CrAT to use choline as the acceptor of the acetyl group instead of its natural substrate carnitine. First, we prepared the CrAT triple mutant T465V/T467N/R518N (TM), which incorporates the reverse substitutions that Cronin successfully performed in rat ChAT and allowed him to accommodate carnitine instead of choline. The triple mutant was expected to eliminate most of the interactions between the enzyme and the carboxylate group of carnitine, which might favor the binding of choline. At the same time, however, this triple mutant might increase the volume of the catalytic site of CrAT, which could interfere with the correct positioning of the smaller choline. Therefore, to reduce the volume of the carnitine binding pocket and create a more favorable environment to accommodate the choline, we prepared the CrAT quadruple mutant A106M/T465V/T467N/R518N (QM) with the additional replacement of Ala[106] with Met. CrAT TM and QM were expressed in *E. coli*, and the protein was purified to homogeneity. Kinetic experiments were performed with the substrate pairs choline/acetyl-CoA and carnitine/acetyl-CoA (Table 3). The wt enzyme and both mutants showed standard saturation kinetics for all of the substrates tested, with the exception of the quadruple mutant with carnitine.

Both CrAT mutants showed improved catalytic efficiency toward choline (K_{cat}/K_m) compared with that of the wt, and this increase was higher in the QM (9-fold) than in the TM (5-fold). In both mutants, the increase in catalytic efficiency was more influenced by the lowering of the K_m value toward

Table 3: Kinetic Parameters of Rat CrAT in *Escherichia coli* Cells Expressing CrAT Wild-Type, Triple Mutant T465V/T467N/R518N and Quadruple Mutant A106M/T465V/T467N/R518N[a]

	K_m (μM)		K_{cat} (s^{-1})		catalytic efficiency (K_{cat}/K_m) ($M^{-1}\cdot s^{-1}$)	
CrAT	carnitine	choline	carnitine	choline	carnitine	choline
wt	101 ± 4.6	86400 ± 5300	86.9 ± 3.6	1.58 ± 0.14	8.6×10^5	18.2
TM	260000 ± 19000	29000 ± 4200	2.97 ± 0.07	2.43 ± 0.10	11.4 ($\downarrow$ 75000)	83.7 ($\uparrow$ 5)
QM	>300000	18100 ± 330	0.98 ± 0.08	3.11 ± 0.19	1.34 ($\downarrow$ 640000)	172 ($\uparrow$ 9)

[a] Purified protein from *E. coli* expressing CrAT wild-type (wt) and mutants T465V/T467N/R518N (TM) and A106M/T465V/T467N/R518N (QM) were assayed for kinetics as described in Experimental Procedures. The results are the mean $\pm$ SD of three independent experiments with different preparations. The values in parentheses represent the fold change of catalytic efficiency (K_{cat}/K_m) versus that of the wild-type.

choline (5-fold in the QM and 3-fold in the TM) than by an increase in the K_{cat} value.

In contrast with the results obtained with choline, the two mutants reduced the catalytic efficiency toward carnitine. Again, the greatest effect occurred with the quadruple mutant, with a decrease of more than 5 orders of magnitude (640 000-fold) in catalytic efficiency in comparison with that of wt, whereas the reduction in the triple mutant was about 75 000-fold. This impairment in catalytic efficiency toward carnitine is due to the combination of a decrease in the K_{cat} value and an increase in the K_m value toward carnitine, the latter being the stronger factor.

The comparison of the catalytic efficiencies between choline and carnitine for each enzyme derivative shows that although CrAT wt prefers carnitine over choline as the acceptor of the acetyl moiety by a factor of 47 000 (8.6 $\times$ 10^5 vs. 18.2 $M^{-1}s^{-1}$) the mutation of four amino acid residues in CrAT shifts the catalytic discrimination of the enzyme in favor of choline. Thus, the QM acetylates choline with a higher catalytic efficiency than carnitine by a factor of 128 (172 vs 1.34 $M^{-1}s^{-1}$).

In the CrAT triple and quadruple mutants, the K_m values for acetyl-CoA in the presence of carnitine and choline were very similar to those of wt CrAT. When carnitine was used, the K_m values for acetyl-CoA were 39 μM for wt CrAT, 33 μM for the TM, and 28 μM for the QM. In the presence of choline, the K_m values for acetyl-CoA were 19 μM for wt CrAT, 26 μM for the TM, and 28 μM for the QM. These results indicate that none of the mutations had any effect on the affinity of the enzyme for acetyl-CoA.

Our results indicate two factors that contribute to the discrimination between choline and carnitine in CrAT to a similar extent. The first factor is the electrostatic interaction of Thr[465] and Arg[518] with the carboxylate group of carnitine. When this interaction is eliminated in the CrAT triple mutant, its catalytic efficiency toward carnitine dramatically decreases, and there is a 5-fold increase in catalytic efficiency toward choline. The second factor is the side-chain volume of the residues around the carnitine in the active site of CrAT. The replacement of Ala[106] in CrAT by methionine in the quadruple mutant reduces the volume of the carnitine binding site, which almost completely blocks carnitine acetyltransferase activity and increases the catalytic efficiency toward choline by 9-fold, nearly doubling the effect of the abolition of the electrostatic interactions.

In an attempt to understand the characteristics of the carnitine/choline binding site in CrAT, 3-D models were built for the wt and the triple and quadruple CrAT mutants and compared with the published structures of rat ChAT (*17*,
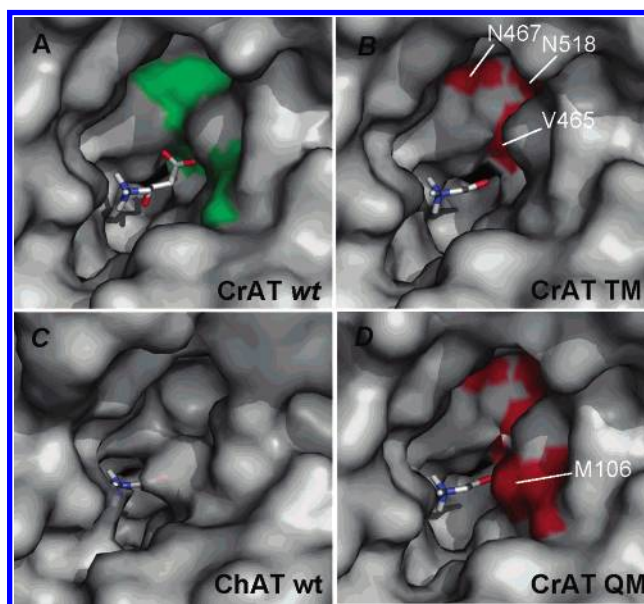

FIGURE 5: Models of substrate binding sites for wt CrAT, CrAT TM, and CrAT QM compared to the active site of rat wt ChAT. The representation of the protein surface of the entrance tunnel for carnitine/choline substrates for (A) rat CrAT wt, (B) CrAT triple mutant (T465V/T467N/R518N), (C) wt ChAT structure, and (D) CrAT quadruple mutant (A106M/T465V/T467N/R518N). The location of a molecule of carnitine is represented in the wt CrAT model, whereas a molecule of choline is represented in CrAT TM, CrAT QM, and wt ChAT. The vacuum electrostatics for active sites was calculated and represented using PyMOL (*33*). The approximate positions of mutated residues Met[106], Val[465], Asn[467], and Asn[518] are indicated in red. Green shows the approximate positions of Ala[106], Thr[465], Thr[467], and Arg[518] in wt CrAT.

18). Using rigid docking techniques, the location of both substrates was calculated for each enzyme active center (Figure 5). According to the models, the electrostatic characteristics of the substrate site for TM CrAT resemble wt ChAT more than wt CrAT. In addition to the lack of specific contact for the carboxylate group of carnitine, the site for the trimethylammonium group, common for both substrates, is maintained. In the quadruple mutant, the presence of Met instead of the original Ala[106] almost completely mimics the wt ChAT active site. We conclude that the reduction of the size of the tunnel impedes the entry of carnitine and allows better positioning of the smaller choline.

The fact that our improvement of the catalytic efficiency of CrAT toward choline (9-fold) was not as successful as that achieved by Cronin (*19*) with ChAT toward carnitine (1620-fold) is not due to a failure in the acquisition of choline activity of CrAT mutants because their catalytic activity with

choline is only 3 times lower than that of mutant ChAT with carnitine (172 vs 469 $M^{-1}s^{-1}$). The discrepancy is attributable to the fact that wt CrAT is very active toward choline (K_{cat}/K_m = 18.2 $M^{-1}s^{-1}$), whereas wt ChAT has a very low carnitine acetyltransferase activity (K_{cat}/K_m = 0.289 $M^{-1}s^{-1}$). The relatively high choline acetyltransferase activity of wt CrAT could be due to the fact that choline can enter the carnitine binding pocket without any steric hindrance. The amino acid substitutions in rat CrAT in this study disclose several residues that are involved in acyl-CoA and choline substrate recognition and provide insight into the molecular requirements for their correct positioning for an efficient catalysis.

The carnitine acyltransferase family has received much attention because they are considered promising targets for the development of drugs against type II diabetes and other human diseases (*31*, *32*). CrAT mutant D356A/M5464G catalyzes acyl-CoAs over a wide range of chain length, from acetyl- to palmitoyl-CoA, thereby mimicking the natural proteins CrAT, COT, and CPT. Long-chain acyl-CoAs (LC-CoAs) are candidate mediators of insulin resistance. Therefore, this double mutant may be useful for studies of the influence of fatty acids on insulin resistance. If this CrAT double mutant were to be overexpressed, these harmful LC-CoAs would be transformed into acylcarnitine derivatives and then excreted in urine, thus detoxifying selective acyl residues and releasing free CoA and modulating the CoA/acyl-CoA ratio. The overexpression of this mutant CrAT presents two advantages over the overexpression of CPT I. First, CrAT mutant D356A/M564G reacts with a broader series of fatty acid acyl-CoAs than CPT I and facilitates the excretion of a wider range of harmful acyl residues as acylcarnitines. Second, CrAT mutant D356A/M5464G activity is not inhibited by malonyl-CoA (data not shown): at variance with wt CPT I but the same as wt CrAT. The results presented in this study not only help us to understand the structure/function relationship within the acyltransferase family, but also facilitate studies on obesity, noninsulin-dependent diabetes (NIDDM), and defective β-oxidation.

ACKNOWLEDGMENT

REFERENCES

1. Miyazawa, S., Ozasa, H., Furuta, S., Osumi, T., and Hashimoto, T. (1983) Purification and properties of carnitine acetyltransferase from rat liver, *J. Biochem. (Tokyo) 93*, 439−451.
2. Miyazawa, S. Ozasa, H., Osumi, T., and Hashimoto, T. (1983) Purification and properties of carnitine octanoyltransferase and carnitine palmitoyltransferase from rat liver, *J. Biochem. (Tokyo) 94*, 529−542.
3. McGarry, J. D., and Brown, N. F. (1997) The mitochondrial carnitine palmitoyltransferase system. From concept to molecular analysis, *Eur. J. Biochem. 244*, 1−14.
4. Bieber, L. L., Krahling, J. B., Clarke, P. R., Valkner, K. J., and Tolbert, N. E. (1981) Carnitine acyltransferases in rat liver peroxisomes, *Arch. Biochem. Biophys. 211*, 599−604.
5. Zammit, V. A. (1999) Carnitine acyltransferases: functional significance of subcellular distribution and membrane topology, *Prog. Lipid. Res. 38*, 199−224.
6. Bieber, L. L. (1988) Carnitine, *Annu. Rev. Biochem. 57*, 261−283.
7. Kalaria, R. N., and Harik, S. I. (1992) Carnitine acetyltransferase activity in the human brain and its microvessels is decreased in Alzheimer's disease, *Ann. Neurol. 32*, 583−586.
8. DiDonato, S., Rimoldi, M., Moise, A., Bertagnoglio, B., and Uziel, G. (1979) Fatal ataxic encephalopathy and carnitine acetyltransferase deficiency: a functional defect of pyruvate oxidation? *Neurology 29*, 1578−1583.
9. Brevetti, G., Angelini, C., Rosa, M., Carrozzo, R., Perna, S., Corsi, M., Matarazzo, A., and Marcialis, A. (1991) Muscle carnitine deficiency in patients with severe peripheral vascular disease, *Circulation 84*, 1490−1495.
10. Melegh, B., Seress, L., Bedekovics, T., Kispal, G., Sümegi, B., Trombitas, K., and Mehes, K. (1999) Muscle carnitine acetyltransferase and carnitine deficiency in a case of mitochondrial encephalomyopathy, *J. Inherited Metab. Dis. 22*, 827−838.
11. An, J., Muoio, D. M., Shiota, M., Fujimoto, Y., Cline, G. W., Shulman, G. I., Koves, T. R., Stevens, R., Millington, D., and Newgard, C. B. (2004) Hepatic expression of malonyl-CoA decarboxylase reverses muscle, liver and whole-animal insulin resistance, *Nat. Med. 10*, 268−274.
12. Jogl, G., and Tong, L. (2003) Crystal structure of carnitine acetyltransferase and implications for the catalytic mechanism and fatty acid transport, *Cell 112*, 113−122.
13. Wu, D., Govindasamy, L., Lian, W., Gu, Y., Kukar, T., Agbandje-McKenna, M., and McKenna, R. (2003) Structure of human carnitine acetyltransferase. Molecular basis for fatty acyl transfer, *J. Biol. Chem. 278*, 13159−13165.
14. Jogl, G., Hsiao, Y., and Tong, L. (2005) Crystal structure of mouse carnitine octanoyltransferase and molecular determinants of substrate selectivity, *J. Biol. Chem. 280*, 738−744.
15. Cordente, A. G., López-Viñas, E., Vázquez, M. I., Swiegers, J. H., Pretorius, I. S., Gómez-Puertas, P., Hegardt, F. G., Asins, G., and Serra, D. (2004) Redesign of carnitine acetyltransferase specificity by protein engineering, *J. Biol. Chem. 279*, 33899−33908.
16. Hsiao, Y., Jogl, G. and Tong, L. (2004) Structural and biochemical studies of the substrate selectivity of carnitine acetyltransferase, *J. Biol. Chem. 279*, 31584−31589.
17. Govindasamy, L., Pedersen, B., Lian, W., Kukar, T., Gu, Y., Jin, S., Agbandje-McKenna, M., Wu, D., and McKenna, R. (2004) Structural insights and functional implications of choline acetyltransferase, *J. Struct. Biol. 148*, 226−235.
18. Cai, Y., Cronin, C. N., Engel, A. G., Ohno, K., Hersh, L. B., and Rodgers, D. W. (2004) Choline acetyltransferase structure reveals distribution of mutations that cause motor disorders, *EMBO J. 23*, 2047−2058.
19. Cronin, C. N. (1998) Redesign of choline acetyltransferase specificity by protein engineering, *J. Biol. Chem. 273*, 24465−24469.
20. Govindasamy, L., Kukar, T., Lian, W., Pedersen, B., Gu, Y., Agbandje-McKenna, M., Jin, S., McKenna, R., and Wu, D. (2004) Structural and mutational characterization of L-carnitine binding to human carnitine acetyltransferase, *J. Struct. Biol. 146*, 416−424.
21. Cronin, C. N. (1997) cDNA cloning, recombinant expression, and site-directed mutagenesis of bovine liver carnitine octanoyltransferase, *Eur. J. Biochem. 247*, 1029−1037.
22. Morillas, M., López-Viñas, E., Valencia, A., Serra, D., Gómez-Puertas, P., Hegardt, F. G., and Asins, G. (2004) Structural model of carnitine palmitoyltransferase I based on the carnitine acetyltransferase crystal, *Biochem. J. 379*, 777−784.
23. Hooft, R. W., Vriend, G., Sander, C., and Abola, E. E. (1996) Errors in protein structures, *Nature 381*, 272.
24. Vriend, G. (1990) WHAT IF: a molecular modeling and drug design program, *J. Mol. Graph. 8*, 52−56.
25. Laskowski, R. A., MacArthur, M. W., Moss, D. S., and Thornton, J. M. (1993) PROCHECK: a program to check the stereochemical quality of protein structures, *J. Appl. Crystallogr. 26*, 283−291.
26. Goodsell, D. S., Morris, G. M., and Olson, A. J. (1996) Automated docking of flexible ligands: applications of AutoDock, *J. Mol. Recognit. 9*, 1−5.
27. Morris, G. M., Goodsell, D. S., Halliday, R. S., Huey, R., Hart, E., Belew, R. K., and Olson, A. J. (1998) Automated docking using a Lamarckian genetic algorithm and an empirical binding free energy function, *J. Comput. Chem. 19*, 1639−1662.
28. Morillas, M., Gómez-Puertas, P., Roca, R., Serra, D., Asins, G., Valencia, A., and Hegardt, F. G. (2001) Structural model of the catalytic core of carnitine palmitoyltransferase I and carnitine octanoyltransferase (COT): mutation of CPT I histidine 473 and

alanine 381 and COT alanine 238 impairs the catalytic activity, *J. Biol. Chem. 276*, 45001−45008.

29. Swiegers, J. H., Dippenaar, N., Pretorius, I. S., and Bauer, F. F. (2001) Carnitine-dependent metabolic activities in *Saccharomyces cerevisiae*: three carnitine acetyltransferases are essential in a carnitine-dependent strain, *Yeast 18*, 585−595.

30. Hassett, R. P., and Crockett, E. L. (2000) Endpoint fluorometric assays for determining activities of carnitine palmitoyltransferase and citrate synthase, *Anal. Biochem. 287*, 176−179.

31. Anderson, R. C. (1998) Carnitine palmitoyltransferase: a viable target for the treatment of NIDDM? *Curr. Pharm. Des. 4*, 1−16.

32. Wagman, A. S., and Nuss, J. M. (2001) Current therapies and emerging targets for the treatment of diabetes, *Curr. Pharm. Des. 7*, 417−450.

33. DeLano, W. L. (2002) *The PyMOL Molecular Graphics System*, DeLano Scientific, San Carlos, CA.